An Initial Event in the Insect Innate Immune Response: Structural and Biological Studies of Interactions between β-1,3-Glucan and the N-Terminal Domain of β-1,3-Glucan Recognition Protein

Huaien Dai,[†] Yasuaki Hiromasa,[†] Daisuke Takahashi,[†] David VanderVelde,[‡,§] Jeffrey A. Fabrick,[†,∥] Michael R. Kanost,[†] and Ramaswamy Krishnamoorthi*,[†]

[†]Department of Biochemistry, Kansas State University, Manhattan, Kansas 66506, United States
[‡]Structural Biology Center, University of Kansas, Lawrence, Kansas 66045, United States

Ⓢ Supporting Information

ABSTRACT: In response to invading microorganisms, insect β-1,3-glucan recognition protein (βGRP), a soluble receptor in the hemolymph, binds to the surfaces of bacteria and fungi and activates serine protease cascades that promote destruction of pathogens by means of melanization or expression of antimicrobial peptides. Here we report on the nuclear magnetic resonance (NMR) solution structure of the N-terminal domain of βGRP (N-βGRP) from Indian meal moth (*Plodia interpunctella*), which is sufficient to activate the prophenoloxidase (proPO) pathway resulting in melanin

formation. NMR and isothermal calorimetric titrations of N-βGRP with laminarihexaose, a glucose hexamer containing β-1,3 links, suggest a weak binding of the ligand. However, addition of laminarin, a glucose polysaccharide (∼6 kDa) containing β-1,3 and β-1,6 links that activates the proPO pathway, to N-βGRP results in the loss of NMR cross-peaks from the backbone $^{15}N-^{1}H$ groups of the protein, suggesting the formation of a large complex. Analytical ultracentrifugation (AUC) studies of formation of the N-βGRP−laminarin complex show that ligand binding induces self-association of the protein−carbohydrate complex into a macro structure, likely containing six protein and three laminarin molecules (∼102 kDa). The macro complex is quite stable, as it does not undergo dissociation upon dilution to submicromolar concentrations. The structural model thus derived from this study for the N-βGRP−laminarin complex in solution differs from the one in which a single N-βGRP molecule has been proposed to bind to a triple-helical form of laminarin on the basis of an X-ray crystallographic structure of the N-βGRP−laminarihexaose complex [Kanagawa, M., Satoh, T., Ikeda, A., Adachi, Y., Ohno, N., and Yamaguchi, Y. (2011) *J. Biol. Chem. 286*, 29158−29165]. AUC studies and phenoloxidase activation measurements conducted with the designed mutants of N-βGRP indicate that electrostatic interactions involving Asp45, Arg54, and Asp68 between the ligand-bound protein molecules contribute in part to the stability of the N-βGRP−laminarin macro complex and that a decreased stability is accompanied by a reduced level of activation of the proPO pathway. An increased level of β-1,6 branching in laminarin also results in destabilization of the macro complex. These novel findings suggest that ligand-induced self-association of the βGRP−β-1,3-glucan complex may form a platform on a microbial surface for recruitment of downstream proteases, as a means of amplification of the initial signal of pathogen recognition for the activation of the proPO pathway.
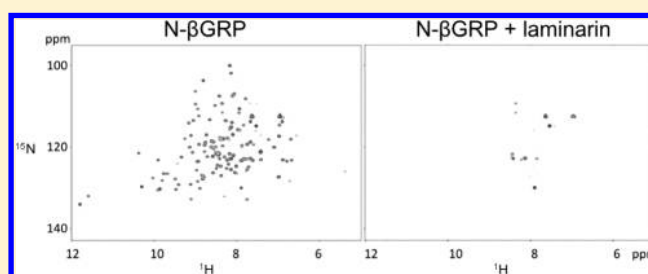
βGRPs, also called Gram-negative bacteria binding proteins (GNBPs), make up a family of insect pathogen recognition receptors that bind to β-1,3-glucan, a structural component of fungal cell walls and bacterial surfaces.[1−6] The protein−carbohydrate binding event triggers activation of serine protease cascades leading to the activation of the proPO pathway in the hemolymph and intracellular Toll signaling.[7,8] The activated proPO pathway produces melanin that encapsulates pathogenic microorganisms, whereas the Toll pathway results in the expression of antimicrobial peptides and/or proteins.

βGRPs share a conserved primary structure comprising an amino-terminal carbohydrate-binding domain (N-βGRP) and a carboxyl-terminal β-1,3-glucanase-like domain. N-βGRP binds to Curdlan, a linear water-insoluble β-1,3-glucan polysaccharide, and to laminarin, a water-soluble β-1,3-glucan polysaccharide containing β-1,6 branches.[1,9] *Plodia interpunctella* N-βGRP mixed with laminarin generates a significant synergistic activation of the proPO pathway.[9] N-βGRP also induces aggregation of microorganisms such as *Saccharomyces cerevisiae* and *Escherichia coli*, albeit less effectively than does the full-length protein.[9] Aggregation of pathogens in vivo may create a superior trigger for activating biochemical cascades of cellular immunity[9] or may provide a platform for the assembly
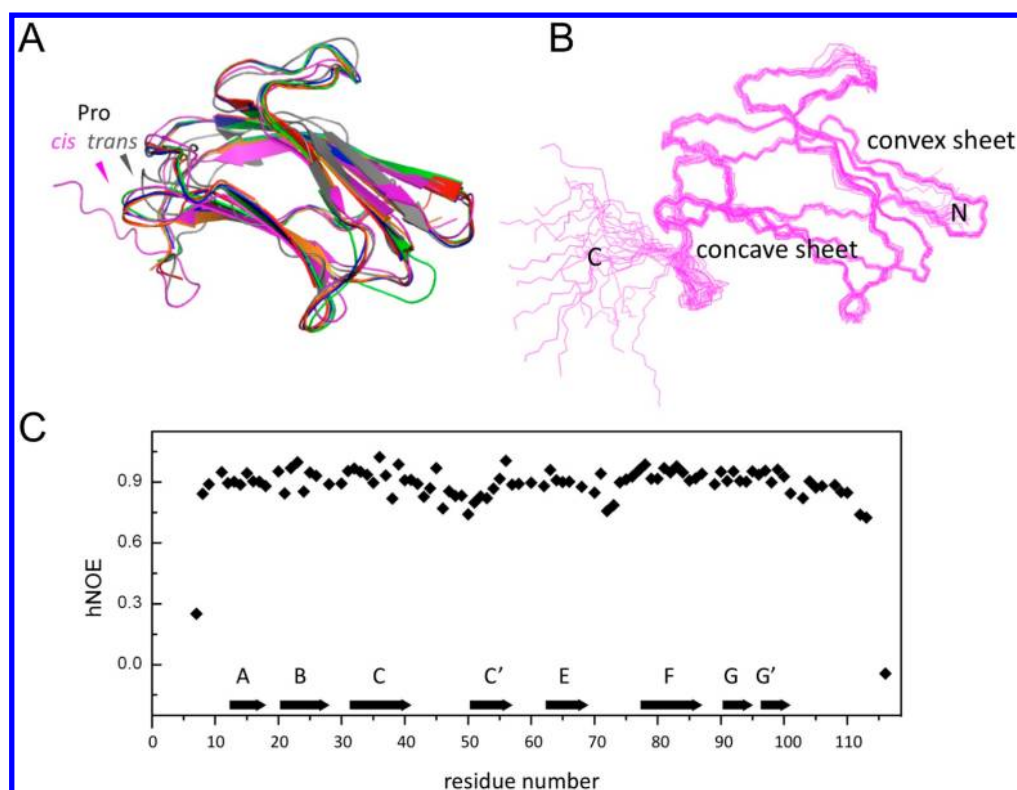
Figure 1. (A) Superimposition of ribbon structures of N-βGRP from several insects: *P. interpunctella* [purple, PDB entry 2KHA, NMR (current work)], *B. mori* (gray, PDB entry 2RQE, NMR[11]), *D. melanogaster* (green, PDB entry 3IE4, X-ray[13]), *B. mori* (laminarihexaose-bound, orange, PDB entry 3AQX, X-ray[12]), *P. interpunctella* (blue, PDB entry 3AQY, X-ray[12]), and *P. interpunctella* (laminarihexaose-bound, red, PDB entry 3AQZ, X-ray[12]). The NMR structure of *P. interpunctella* N-βGRP reported here differs from that of the *B. mori* protein[11] in the conformation of a Pro, as indicated. (B) Ensemble of the 20 lowest-energy structures of *P. interpunctella* N-βGRP (PDB entry 2KHA). (C) Plot of backbone heteronuclear {^{15}N}−^{1}H NOE values vs residue number for *P. interpunctella* N-βGRP. Pro residues do not give rise to {^{15}N}−^{1}H NOEs. A couple of C-terminal residues had hetero-NOE peak intensities barely above the noise level. Each β-strand is represented by an arrow.

of effector complexes.[10] Gaining insight into the molecular mechanism of such pathogen recognition events requires, as a first step, characterization of the structural basis and consequences of binding of β-1,3-glucan by N-βGRP.

Three-dimensional structures have been reported for N-βGRP from three insect species, *Bombyx mori*,[11,12] *Drosophila melanogaster*,[13] and *P. interpunctella*:[12] all three N-βGRPs adopt a common immunoglobulin-like fold with two sheets forming a β-sandwich (Figure 1A). However, different models have been proposed for the binding of β-1,3-glucan by N-βGRP. In the model based on the solution structure of *B. mori* N-βGRP, as determined by means of nuclear magnetic resonance (NMR) spectroscopy, the β-1,3-glucan binding site is located on the concave sheet (strands A, B, and E),[11] while in the models based on the X-ray crystal structure of ligand-free *D. melanogaster* GNBP3 N-domain[13] and that of *P. interpunctella* N-βGRP complexed with laminarihexaose,[12] the binding site is confined to the convex sheet (strands C, C′, F, G, and G′). Furthermore, these three models do not provide any clues for understanding the molecular basis of the synergistic activation of the proPO pathway by β-1,3-glucan and N-βGRP.

In this work, we describe the NMR solution structure determination of *P. interpunctella* N-βGRP (N-terminal region of 118 residues) and mapping of the β-1,3-glucan binding site. We have characterized the binding of laminarihexaose, and that of laminarin, to N-βGRP by NMR, isothermal titration calorimetry (ITC), analytical ultracentrifugation (AUC) studies, site-directed mutagenesis, and prophenoloxidase

activity measurements. Our results demonstrate, for the first time, ligand-induced self-association of the N-βGRP−β-1,3-glucan complex. This process has a significant contribution from electrostatic interactions between N-βGRP molecules in the complex. A reduction in the extent of self-association between N-βGRP−β-1,3-glucan complex molecules leads to a decrease in the rate of proPO activation by the macro complex. Thus, it is suggested that formation of such a protein−carbohydrate macro complex is a structural initiation signal for serine protease cascade activation of the insect immune response and a likely prerequisite for aggregation of micro-organisms.

■ MATERIALS AND METHODS

Materials. Laminarin from *Laminaria digitata* was purchased from Sigma-Aldrich (catalog no. L9634, St. Louis, MO), and its β-1,3 to β-1,6 cross-link number ratio was 7.[14] Laminarihexaose and Curdlan (a water-insoluble β-1,3-glucan) were from Megazyme (Wicklow, Ireland). A much more branched laminarin from *Eisenia bicyclis* with a β-1,3 to β-1,6 cross-link number ratio of 3[15] was purchased from Tokyo Chemical Industry (Tokyo, Japan).

Protein Expression and Purification. The DNA sequence of *P. interpunctella* N-βGRP was cloned via *Bam*HI/*Hin*dIII sites into the Invitrogen pPROEX HTb plasmid.[9] The resulting recombinant protein contains an N-terminal hexahistidine tag followed by a TEV protease cleavage site before the N-βGRP sequence. Expression and purification of His$_6$-N-

βGRP were performed as described previously[9] with a slight modification. His$_6$-N-βGRP was expressed in *E. coli* BL21 cells by induction with isopropyl β-D-thiogalactopyranoside and purified using a Ni^{2+} affinity column. The hexahistidine tag was cleaved by incubating His$_6$-N-βGRP with His$_6$-TEV protease (GE Helthcare), and the resultant mixture was passed through a Ni^{2+} affinity column to remove the cleaved hexahistidine tag, the TEV protease, and uncleaved protein. The purity of N-βGRP was confirmed by sodium dodecyl sulfate−polyacrylamide gel electrophoresis (SDS−PAGE), and the amino acid sequence of recombinant N-βGRP was confirmed by mass spectrometry. The recombinant protein had five extra N-terminal and seven extra C-terminal residues from the vector used. Proteins uniformly labeled either with ^{15}N or with both ^{13}C and ^{15}N were produced by growing *E. coli* in M9 medium containing [^{15}N]ammonium chloride and either D-glucose or uniformly ^{13}C-labeled D-glucose (Cambridge Isotope Laboratories), respectively.

N-βGRP containing a D45A or D45K mutation was prepared according to the instructions of the QuikChange mutagenesis kit (Stratagene). The mutation was confirmed by DNA sequencing and mass spectrometry of the purified protein.

NMR Spectroscopy. A typical solution sample of N-βGRP used for three-dimensional NMR experiments consisted of 1.7−2.0 mM uniformly ^{13}C- and ^{15}N-labeled protein in 20 mM sodium phosphate buffer (pH 6.5). NMR data were collected at 25 °C using a Bruker Avance 800 MHz spectrometer equipped with a cryogenic probe at the Structural Biology Center of the University of Kansas. The data sets were processed using NMRPipe[16] and analyzed using Sparky.[17] A series of standard two-dimensional (2D) and three-dimensional (3D) NMR spectra were collected for backbone and side chain resonance assignments and structural constraint measurements.[18] These include 2D ^{15}N HSQC and ^{13}C HSQC, 3D CBCA(CO)NH, HNCACB, HN(CO)CA, HNCA, CCCONH, HCCCONH, HCCH-TOCSY, ^{15}N-edited TOCSY, ^{15}N-edited NOESY, and ^{13}C-edited NOESY. An additional 3D ^{15}N-edited NOESY-HSQC data set was gathered from the ^{15}N-labeled sample to identify HN−HN contacts. Sequence-specific backbone ^{1}H, ^{15}N, and ^{13}C resonance assignments were made from an analysis of the 3D NMR data sets, CBCA(CO)NH, HNCACB, HN(CO)CA, and HNCA. Side chain resonances were assigned using 3D CCCONH, HCCCONH, HCCH-TOCSY, and ^{15}N-edited TOCSY data. Unambiguous NOE constraints were manually assigned using 3D ^{15}N-edited and ^{13}C-edited NOESY spectra. Dihedral constraints for the backbone torsion angles (φ and ψ) were obtained using TALOS.[19] Hydrogen bond constraints were employed for β-stand regions based on the NOE patterns and the chemical shift index prediction of the secondary structure.[20] Structures of N-βGRP were calculated by a simulated annealing procedure using CNS.[21] One hundred structures were calculated, from which the 20 lowest-energy structures were chosen for the final structural ensemble.

For NMR titration experiments, 2D ^{1}H−^{15}N HSQC spectra of 0.5−1.0 mM ^{15}N-labeled N-βGRP in 20 mM sodium phosphate buffer (pH 6.5) were collected at 25 °C. Laminarihexaose or laminarin solutions (3 and 1 mM, respectively) were prepared in the same buffer and then added stepwise to the protein sample (0.5 mM). The chemical shift difference between ligand-free and ligand-saturated protein was calculated for each backbone NH group as $\{[\Delta H^2 + (\Delta N/5)^2]/2\}^{1/2}$.

Fluorescence Spectroscopy. Fluorescence emission spectra were recorded with a Cary Eclipse fluorescence spectrophotometer (Varian, Inc.) equipped with dual monochromators. The experiments were performed using a 1 cm path length 3.5 mL quartz cuvette. The samples were excited at 295 nm, and emission was measured between 300 and 400 nm to monitor Trp fluorescence.

Analytical Ultracentrifugation. Sedimentation velocity experiments were conducted with an Optima XL-I ultracentrifuge (Beckman Coulter, Inc., Brea, CA) using an An-60 Ti rotor at 20 °C with 50 mM Tris-HCl (pH 7.3) buffer containing 50 mM NaCl.[22] Sedimentation was monitored by absorbance or interference optics using double-sector aluminum cells with a final loading of 400 μL per sector. Sedimentation was performed at 49000 rpm with scans taken at 5 min intervals. Data were analyzed using DCDT+ version 1.16 (http://www.jphilo.mailway.com). Sedimentation coefficients were calculated using $g(s^*)$ and dc/dt fitting functions in DCDT+. The buffer density and viscosity were calculated with SEDNTERP version 1.08 (http://www.jphilo.mailway.com). Bovine serum albumin (BSA) was used as a standard to account for effects of changes in solution density and viscosity when high concentrations of laminarin or laminarihexaose were used. The partial specific volume of a protein was calculated from its amino acid composition using SEDNTERP (0.7306 mL/g for N-βGRP at 20 °C). The partial specific volume used for laminarin was 0.622 mL/g.[23]

Isothermal Titration Calorimetry. ITC measurements were taken using the MCS-ITC system (MicroCal, Northampton, MA) at 30 °C.[24] Recombinant N-βGRP and laminarin solutions were dialyzed overnight at 4 °C against 50 mM Tris-HCl (pH 7.5) buffer containing 50 mM NaCl. Laminarihexaose was directly dissolved in the buffer. All solutions were degassed before being used. A typical experiment consisted of 20 injections of 10 μL of a laminarin or laminarihexaose solution (1.67 mM) into 1.38 mL of a protein solution. The heat of dilution of the laminarin or laminarihexaose solution upon injection into the buffer solution was subtracted from the experimental titration data. Baseline corrections and integration of the calorimeter signals were performed using Origin (MicroCal).

Curdlan Pull-Down Assay. The procedure described by Fabrick et al.[9] was employed. Briefly, for each assay, 20 μg of purified protein (wide-type βGRP-N, D45A, or D45K) was incubated with 0.5 mg of Curdlan for 10 min. The protein/Curdlan mixture was centrifuged at 10000g for 5 min, and the supernatant corresponding to the unbound fraction was saved. The bound protein was eluted from Curdlan when the mixture was heated at 95 °C for 5 min in SDS sample buffer. Equal volumes of purified, unbound, and bound proteins were analyzed by SDS−PAGE with Coomassie blue staining.

Activation of the ProPO Pathway. A method described by Ma and Kanost[2] and Fabrick et al.[4] was used, incorporating the modified protocol recently developed by Laughton and Siva-Jothy[25] to follow proPO activation in the absence or presence of laminarin. Briefly, 10 μL of recombinant proteins (0.4 mg/mL) was incubated with 5 μL of buffer or laminarin (10 mg/mL) and mixed with 5 μL of *Manduca sexta* plasma. The volume of each sample well was increased to 130 μL with sodium phosphate buffer (pH 6.8). After incubation for 15 min at room temperature, 20 μL of 30 mM dopamine hydrochloride was added and phenoloxidase activity was determined by measuring absorbance at 490 nm. The phenoloxidase activity
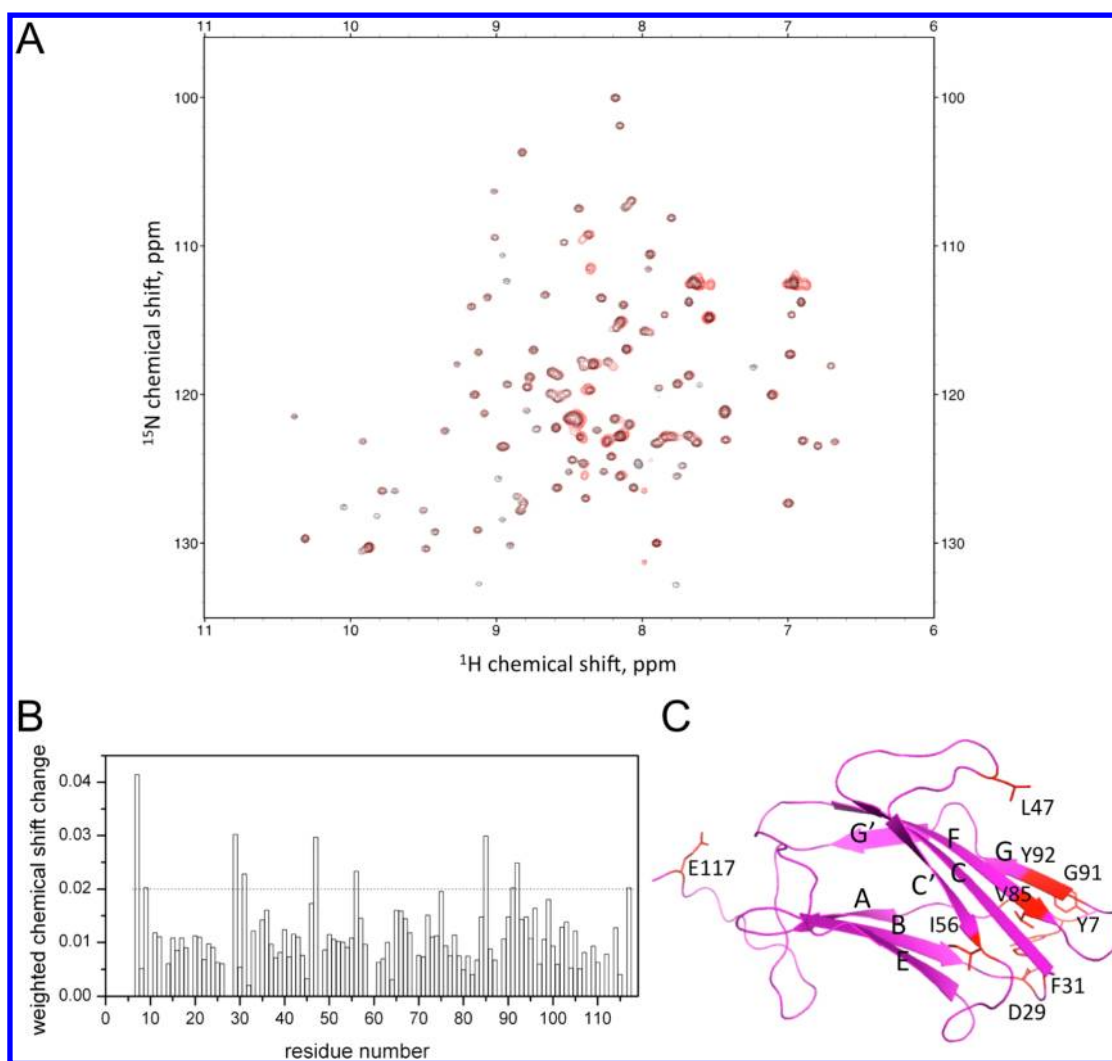
Figure 2. Mapping of the ligand binding site on *P. interpunctella* N-βGRP by NMR titration of laminarihexaose at 25 °C and pH 6.5. (A) ^{1}H−^{15}N HSQC spectra of N-βGRP (0.5 mM) in the absence (black) or presence (red) of laminarihexaose (3 mM). (B) Chemical shift changes undergone by the backbone ^{15}N−^{1}H groups. The weighted average of chemical shift changes of an ^{15}N−^{1}H group was calculated by using the formula $\{[\Delta H^2 + (\Delta N/5)^2]/2\}^{1/2}$, where ΔH and ΔN represent ^{1}H and ^{15}N chemical shift changes, respectively. (C) Residues undergoing a chemical shift perturbation of >0.02 ppm upon laminarihexaose titration are colored red.

was presented as the change in milli-absorbance unit per minute. Statistical analysis was performed using Prism 5 (GraphPad Software).

RESULTS AND DISCUSSION

Homogeneity of N-βGRP. The homogeneity of extensively purified N-βGRP was characterized by AUC. The sedimentation analysis of N-βGRP exhibited a homogeneous species with an $S_{20,w}$ value of 1.90 S, corresponding to a weight-average molecular mass of 14500 Da by dc/dt analysis, a value in good agreement with the calculated mass of 14601 Da. The N-βGRP sedimentation pattern remained the same for a 1.7 mM solution (data not shown), thus indicating that N-βGRP existed as a monomer in solution at concentrations used for NMR experiments.

N-βGRP Solution Structure and Mapping of the β-1,3-Glucan Binding Site. The monomer structure of N-βGRP was determined using solution NMR methods (Figure 1B). The chemical shifts of backbone and side-chain ^{1}H, ^{15}N, and ^{13}C nuclei of the backbone were assigned by the application of standard multidimensional heteronuclear NMR methods.[26]

The upfield Cγ chemical shift and downfield Cβ chemical shift of Pro19, together with the strong NOE correlation between its Hα and Hα of the preceding Tyr18, indicate that the peptide bond between Tyr18 and Pro19 adopts a *cis* conformation, consistent with the reported crystal structures,[12,13] but in contrast to the *trans* conformation reported for the corresponding Pro in the solution structure of *B. mori* N-βGRP.[11] The heteronuclear steady-state $\{^{15}N\}-^1$H NOE values are sensitive to the dynamics of the peptide N−H bonds on a subnanosecond time scale.[27] For residues Val8−Thr110, the average value of the heteronuclear NOE is 0.84. The decreased NOE values observed for the N- and C-terminal regions reflect their relatively increased flexibility (Figure 1C).

Structural statistics for the 20 lowest-energy structures are summarized in Table 1 of the Supporting Information. We have identified the eight β-strands according to the standard immunoglobulin nomenclature.[28] Three β-strands, A (Lys13−Ile17), B (Gly21−Pro27), and E (Arg63−Asp68), comprise the concave sheet; β-strands C (Ser32−Leu40), C′ (His51−Ile56), F (Lys78−Ile86), G (Gly91−Gln94), and G′ (Gly97−Thr100)
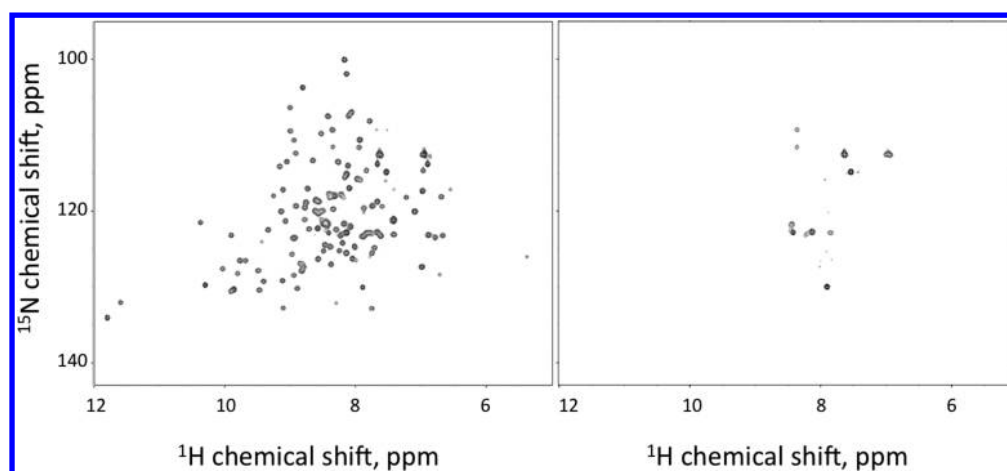
Figure 3. ^{1}H−^{15}N HSQC spectra of N-βGRP (0.5 mM) in the absence (left) or presence (right) of laminarin (1 mM) at 25 °C and pH 6.5.

comprise the convex sheet. Strands G and G′ are split by a kink (Asp95 and Gln96).

Two long loops, C−C′ and E−F, have relatively higher flexibility than the strands as indicated by their slightly lower heteronuclear NOE values. However, the large number of inter-residue ^{1}H−^{1}H NOE distance constraints observed for residues in these two loops indicates that the loops are ordered and fairly rigid (Figure 1B) and hence are unlikely to undergo a large conformational change suggested by Mishima et al.[13] Furthermore, we measured the intensity of fluorescence emitted by tryptophans, among which Trp81 is located on strand F and shielded by the C−C′ loop, before and after the addition of laminarin to the protein sample, and found no change, thus ruling out any conformational changes for the C−C′ and E−F loops caused by laminarin binding. Interestingly, the crystal structure of *P. interpunctella* N-βGRP complexed with laminarihexaose[12] also shows no conformational alteration for these loops.

The effect of β-1,3-glucan binding on N-βGRP structure was characterized by titrating laminarihexaose, a β-1,3-linked glucose hexamer, into a solution of N-βGRP and monitoring the NMR cross-peaks of the protein backbone ^{15}N−^{1}H groups (Figure 2A,B). The perturbed residues are mainly localized on the convex sheet (Figure 2C), consistent with the hexasaccharide binding site identified in the crystal structure of the N-βGRP−laminarihexaose complex.[12] The crystal structure shows that this region interacts with three laminarihexaose molecules, which led the authors to propose that N-βGRP binds to a triple-helical structure of laminarin.[12] However, to date no structural data are available for laminarin, which is a branched polysaccharide. The X-ray fiber diffraction data collected for the linear β-1,3-polysaccharide, Curdlan, have been interpreted to be indicative of a single- or triple-helix structure, depending upon the hydration state of the polysaccharide.[29,30] In the presence of water, the diffraction data have been shown to be consistent with only a single-helix structure.[29]

ITC experiments did not detect any heat exchange for the titration of laminarihexaose (up to 1.6 mM) into N-βGRP (78 μM) (data not shown). This result is consistent with weak laminarihexaose−N-βGRP interactions, as suggested by the NMR data (Figure 2A,B).

Interactions between N-βGRP and Laminarin. Laminarin is a water-soluble oligosaccharide containing both β-1,3 and β-1,6 glycosidic bonds, and the number of β-1,6 glycosidic bonds varies depending upon the source. *L. digitata* laminarin

used in this work has a β-1,3/β-1,6 glycosidic bond ratio of 7.[14] It shows a broad mass distribution (up to 7505 Da) with major mass spectral peaks in the 3932−4580 Da region as obtained by MALDI-TOF mass spectrometry (Figure 1 of the Supporting Information), consistent with the work of Barral et al.[31] Sedimentation velocity analysis of laminarin gave an $S_{20,w}$ value of 1.02 S, which yielded an apparent molecular mass of 4.5 kDa by dc/dt analysis. At a high concentration (5 mg/mL), laminarin had a similar S value, which suggests that laminarin does not associate or aggregate by itself. Young et al. determined an average molecular mass of 7700 Da for laminarin from light scattering experiments.[32] For the purpose of calculating molarities of laminarin solutions used in our work, we adopted a value of 6 kDa for the molecular mass, as provided by the supplier (Sigma-Aldrich).

When laminarin was titrated into N-βGRP, nearly all the cross-peaks in the ^{1}H−^{15}N HSQC spectrum broadened to a noise level (Figure 3). The NMR sample still remained clear with no precipitation. These observations indicate that in the presence of laminarin, N-βGRP forms a higher-order, water-soluble structure. The results also suggest that the binding site identified for laminarihexaose could interact with the surface structure of a carbohydrate polymer. The few cross-peaks that still remained after addition of laminarin to N-βGRP arise from flexible side chain NH groups and peptide NH groups of some terminal residues.

Binding of laminarin to N-βGRP was characterized using ITC (Figure 2 of the Supporting Information). Because of the heterogeneity in laminarin as well as self-association of the resulting protein−:carbohydrate complex, a likely cooperative process, the ITC data, although very similar to those of earlier studies,[12,13] were not fit to any simple binding equilibrium. Qualitatively, the ITC data provided evidence of the binding of laminarin by N-βGRP, an exothermic process.

Interaction between N-βGRP and laminarin was characterized by sedimentation velocity analysis using absorption optics, which detects the distribution of the protein (Figure 4). As the concentration of laminarin added to a fixed concentration of N-βGRP (26.2 μM) increased from 8.3 to 24.9 μM, the concentration of free N-βGRP at 1.9 S decreased and a broad peak appeared between 4 and 9 S. With a further increase in laminarin concentration (83.3 μM), nearly all of the N-βGRP bound to laminarin and a major peak appeared at 5.5 S. A 20-fold excess of laminarin (1.87 mM) caused a slight decrease in the S value (5.1 S) with a shoulder at ∼8 S. A $g(s^*)$
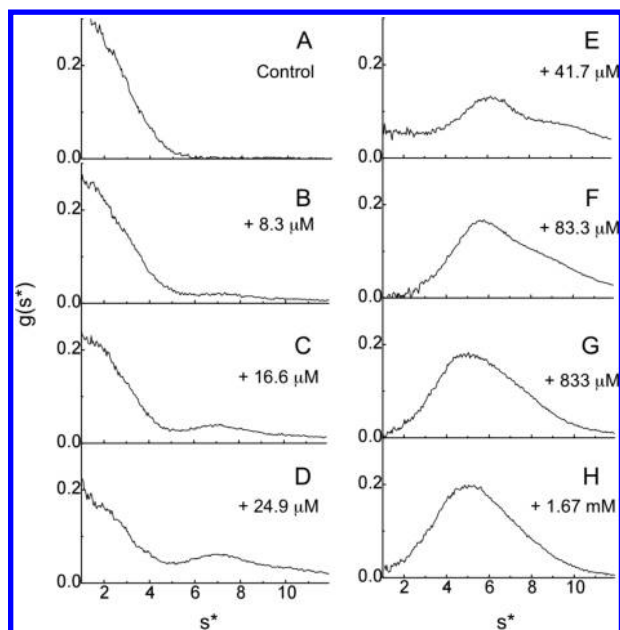
Figure 4. Effect of addition of varying concentrations of laminarin on N-βGRP, as monitored by sedimentation velocity experiments: Sedimentation profiles of N-βGRP (26.2 μM) in the absence (A) or presence of different levels of laminarin (B−H). Sedimentation at 49000 rpm and 20 °C was monitored by measuring absorbance at 280 nm.

fitting analysis yielded an average molecular mass of ∼95 kDa for the 5.5 S species, a value that is remarkably greater than would be expected for a complex that contains one molecule of N-βGRP and three molecules of laminarin. Laminarin contains at least 30 glucose units, and thus, each laminarin molecule could bind multiple N-βGRP molecules. However, the sedimentation profile around the 5.5 S region changed only in a limited way even after addition of a 20-fold excess of laminarin (1.87 mM). This suggests that formation of the 5.5 S species involves not only protein−carbohydrate interactions but also protein−protein interactions. Because N-βGRP or laminarin alone does not oligomerize in solution, these results indicate that binding of laminarin causes self-association of the N-βGRP−laminarin complex. On the basis of the sedimentation coefficient rule,[33] which equates the ratio of average molecular masses of two proteins to the ratio of their sedimentation coefficients raised to the power of $^3/_2$, the shoulder at ∼8 S may be attributed to a higher-order complex that is approximately twice the size of the 5.5 S macro complex. Similar association profiles were observed for the titration of laminarin into *M. sexta* N-βGRP (data not shown).

AUC experiments were similarly performed to monitor the effect of laminarihexaose on N-βGRP (Figure 3 of the Supporting Information). When 54 μM N-βGRP was mixed with 1.0 mM laminarihexaose, the $g(s^*)$ versus s^* plot of N-βGRP displayed no significant change, consistent with weak binding of the ligand. At a higher concentration of the mixture, 234 μM N-βGRP and 14.1 mM laminarihexaose, a faster sedimenting species appeared in the 3−5 s^* region, and with 1.4 mM N-βGRP and 26 mM laminarihexaose, the sedimentation profile shifted further to a higher s^* region. The s^* value range (3−5 S) of the faster sedimenting species falls close to that of BSA (66.5 kDa, 4.3 S). These results suggest that high concentrations of laminarihexaose can mildly induce self-association of the N-βGRP−laminarihexaose

complex. It is of interest to note that *D. melanogaster* GNBP3 N-terminal domain does not bind to laminaritetraose,[6] laminariheptaose, or laminarihexaose.[13] In contrast, several glucan-binding modules belonging to families other than CBM39, to which N-βGRP belongs, possess high binding affinities for hexasaccharides.[34]

Self-Association of the N-βGRP−Laminarin Complex. The stability of the macro assembly of the N-βGRP−laminarin complex was assessed by dilution analysis. AUC experiments (Figure 5) with three different concentrations of N-βGRP at a
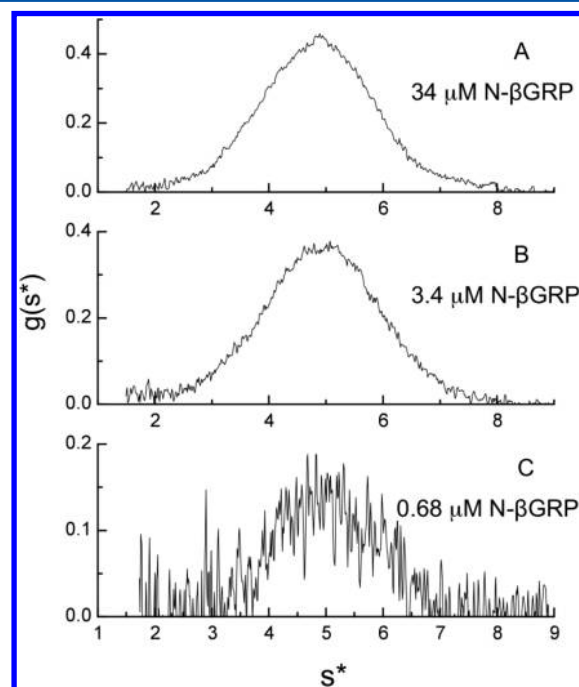

Figure 5. Effect of dilution on the N-βGRP−laminarin complex as monitored by sedimentation velocity profiles: (A) 34 μM N-βGRP and 780 μM laminarin at 280 nm, (B) 3.4 μM N-βGRP and 78 μM laminarin at 220 nm, and (C) 0.68 μM N-βGRP and 15.6 μM laminarin at 205 nm. The N-βGRP/laminarin concentration ratio was maintained at 1/22.9. Sedimentation was conducted at 49000 rpm and 20 °C.

constant N-βGRP/laminarin ratio of 1/22.9 reveal that the s^* profile of the N-βGRP−laminarin complex was unchanged at 5 S even after 50-fold dilution (from 34.0 to 0.68 μM protein). This result indicates that the macro complex does not undergo dissociation at submicromolar concentrations because of strong protein−protein and protein−carbohydrate interactions. Sedimentation velocity experiments were also performed with the more branched *Ei. bicyclis* laminarin (Figure 4 of the Supporting Information). While 83.3 μM *L. digitata* laminarin with a β-1,3/β-1,6 ratio of 7 was sufficient for nearly complete conversion of N-βGRP (26 μM) into the 5.5 S protein−carbohydrate macro complex, a much higher concentration (0.8 mM) of *Ei. bicyclis* laminarin with a β-1,3/β-1,6 ratio of 3 was required for formation of the macro complex. We infer that an increased level of β-1,6 branching reduces the carbohydrate binding strength of N-βGRP and thus the stability of the protein−carbohydrate macro complex.

To determine the stoichiometry of the N-βGRP−laminarin complex, we performed sedimentation velocity analysis using interference optics. The sedimentation of both N-βGRP and laminarin could be monitored, as these water-soluble molecules

affect the refractive index of the solution. Fringe displacements caused by sedimentation provide a measure of the weight concentration of sedimenting species.[35] Sedimentation boundaries were compared between 75 μM N-βGRP and a mixture of 75 μM N-βGRP and 125 μM laminarin (Figure 6). Fringe
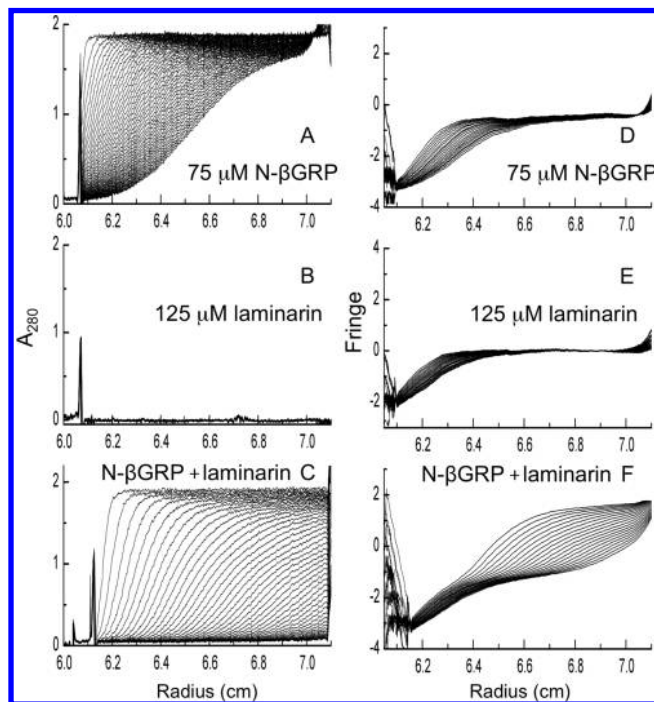

Figure 6. Sedimentation velocity profiles for N-βGRP, laminarin, and their mixtures, as monitored at 49000 rpm and 20 °C by absorbance at 280 nm (A−C) and interference optics (D−F) at 5 min intervals. N-βGRP at 75 μM (A and D) and laminarin at 125 μM (B and E) were sedimented separately or together (C and F). Fringe displacements in panels D−F are given in arbitrary units.

displacement of N-βGRP alone was 2.5 arbitrary units, and that of the N-βGRP−laminarin complex (faster species than either N-βGRP or laminarin alone) was 2.9. By using refractive indices of protein $[(dn/dc) \times 10^3 = 0.186$ mL/mg] and dextran $[(dn/dc) \times 10^3 = 0.151$ mL/mg], the N-βGRP/laminarin weight ratio in the complex was calculated to be approximately 1/0.20, which equals 2/0.92 as a molar ratio. This is consistent with each laminarin (L) molecule binding two N-βGRP (P) molecules to form a P$_2$L complex. Thus, the 5.5 S species is likely to be a trimer of P$_2$L [∼102 kDa (Figure 7A)].

Biological Implication of Self-Association of the N-βGRP−Laminarin Complex. Earlier work[9] has established that N-βGRP and laminarin produce a pronounced synergistic activation of the proPO pathway. Formation of a macro assembly of the protein−:carbohydrate complex in solution, as characterized in this work, likely allows for ready recruitment of circulating βGRP molecules in the hemolymph to initiate protease cascades that function in defense against invading pathogens. The nature of protein−protein interactions present in the complex may be gleaned from a pseudoquadruplex observed in the crystal structure of the N-βGRP−laminarihexaose complex.[12] In the unit cell, N-βGRP molecules pack in a side-by-side fashion because of strong electrostatic attractions such that the tip of the loop connecting strands C and C′ of one molecule fits into a cleft formed between strands C′ and E of another molecule. This structural arrangement is stabilized
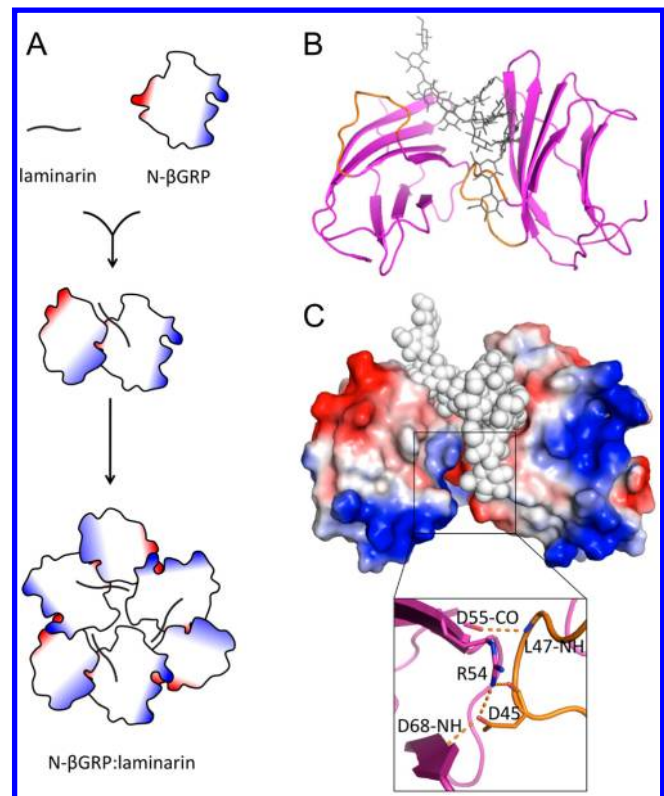

Figure 7. Schematic representation of formation of the N-βGRP−β-1,3-glucan macro complex: (A) Laminarin binding to N-βGRP and self-association of the N-βGRP:laminarin complex. (B and C) N-βGRP packing and concomitant electrostatic interactions as can be observed in the crystal structure of the N-βGRP−laminarihexaose complex.[12] Negative and positive potential surfaces are colored red and blue, respectively.

predominantly by the hydrogen bonds and the salt bridge formed between Leu47 and Asp45 of one protein molecule and Asp55, Arg54, and Asp68 of another (Figure 7B,C).

To test the hypothesis that these electrostatic interactions play a role in the formation of the protein−carbohydrate macro complex, we selected Asp45 for mutagenesis because it makes a hydrogen bond with Asp68 and a salt bridge with Arg54 of another protein molecule through its side chain carboxyl group (Figure 7C, inset). The sedimentation profiles of N-βGRP and mutants D45A and D45K reveal that the complex formed with D45K shifted to 4 S compared to the 5 S complex formed with the wild-type protein. On the other hand, the protein−laminarin macro complex formed by the D45A mutant does not show any change relative to the wild-type complex. These results indicate that in the D45K mutant, electrostatic repulsion between positively charged Lys45 and Arg54 on one hand, and the absence of a hydrogen bond between Lys45 and Asp68 on the other, perturb formation of the protein−carbohydrate macro complex. Clearly, other protein−protein and protein−carbohydrate interactions contribute significantly to the stability of the protein−carbohydrate macro complex, as the D45A mutant shows no alteration in its ability to interact with laminarin and make the protein−carbohydrate macro complex, as compared to that of the wild-type protein. It is of interest to note that while Arg54 is conserved in the three-dimensional structures of N-βGRPs from *P. interpunctella*, *B. mori*, and *D. melanogaster*, Asp45 in *P. interpunctella* N-βGRP is replaced by a Glu in the other two species (Figure 1A).
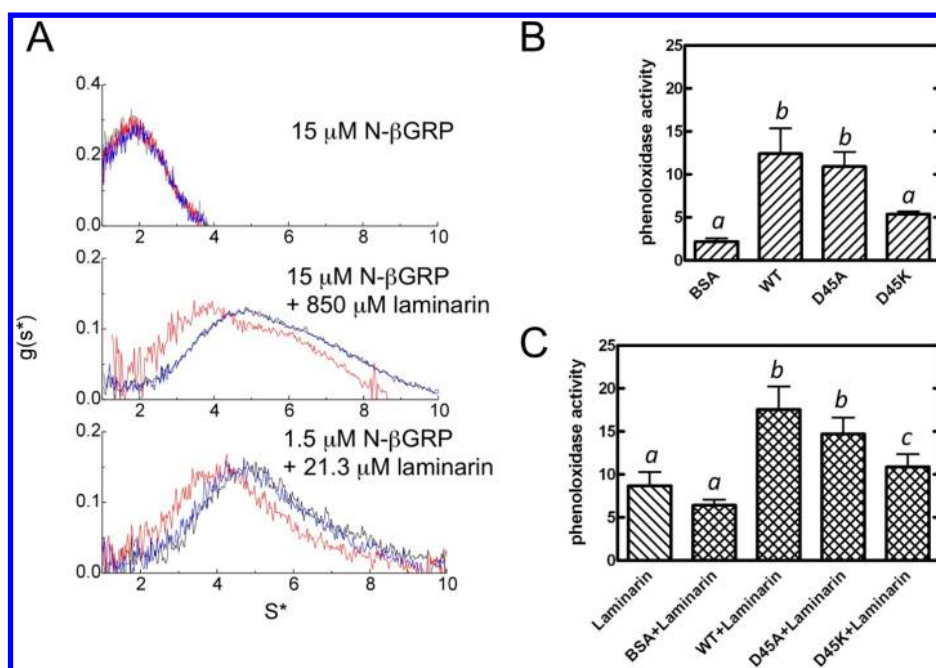
Figure 8. Electrostatic interactions play a role in the formation of the N-βGRP−β-1,3-glucan macro complex. (A) Sedimentation velocity profiles for N-βGRP (wide type, black; D45A, blue; and D45K, red) in the presence of laminarin. (B and C) Activation of the prophenoloxidase pathway by N-βGRP and mutants without (B) or with laminarin (C). Samples of plasma (5 μL) were mixed with protein alone or with protein and laminarin. After incubation at room temperature for 15 min, phenoloxidase activity was measured using dopamine hydrochloride as a substrate, as described in Materials and Methods. The bars represent the means ± the standard error of data from three sets of measurements on a pooled plasma sample. Bars labeled with different letters (*a*, *b*, and *c*) are significantly different [analysis of variance (ANOVA); $p < 0.05$].

β-1,3-Glucan binding activities of D45A and D45K mutants were compared with that of the wild-type protein by Curdlan pull-down assay and ITC with laminarin (Figure 2 of the Supporting Information). Neither of these mutations has any effect on carbohydrate binding activity. Thus, it is concluded that the electrostatic attractions involving Asp45 (Figure 7C), as deduced from the crystal structure of the N-βGRP−laminarihexaose complex,[12] contribute to the self-association of the N-βGRP−laminarin complex.

The functional significance of formation of the protein−carbohydrate macro complex was characterized by measuring proPO activation in insect blood plasma by the wild-type and mutant N-βGRPs in the absence and presence of laminarin (Figure 8B,C). The D45K mutation decreased the level of proPO activation both in the absence of and, to a smaller extent, in the presence of laminarin, while the D45A mutation showed no change, consistent with the AUC data (Figure 8A).

Formation of a macro structure of the βGRP−β-1,3-glucan complex, a likely cooperative process, might present a repeating pattern and thus provide an effective platform for initiating innate immune responses.[36,37] Such an arrangement is reminiscent of peptidoglycan recognition by insect peptidoglycan recognition proteins (PGRPs).[38] It is also of interest to note that some lectins that have a low binding affinity for monosaccharides increase their affinities significantly for oligosaccharides by forming a cluster of lectin−oligosaccharide complexes.[39]

This study thus presents a three-dimensional solution structure of *P. interpunctella* N-βGRP that is highly similar to its crystal structure,[12] provides supporting evidence for the laminarihexaose binding site, presents data for a novel mechanism of proPO activation in the insect immune response that involves self-association of the initial protein−carbohydrate complex, and finally demonstrates the biological relevance of this important step.

CONCLUSIONS

Biophysical characterization of interactions among laminarin, a β-1,3-glucan, and N-terminal domains of insect βGRPs in solution has led to the novel finding that a stable macro complex results from self-association of the initially formed N-βGRP−laminarin complex. Electrostatic interactions between bound protein molecules in the macro complex contribute to its stability and ability to influence the rate of activation of the prophenoloxidase pathway. An increase in the level of β-1,6 branching of laminarin reduces the carbohydrate's βGRP binding affinity. Macro protein−carbohydrate complexes appear to provide an efficient means for recruiting immune response proteins and thus amplifying the initial response.

ASSOCIATED CONTENT

⑤ Supporting Information

A table of statistics for a structural ensemble of the 20 lowest-energy structures of *P. interpunctella* N-βGRP, MALDI mass spectrum of laminarin, β-1,3-glucan binding activities of N-βGRP and mutants as measured by a Curdlan pull-down assay and isothermal titration calorimetry, $g(s^*)$ profiles of sedimentation velocity studies of N-βGRP in the presence of varying amounts of laminarihexaose, and sedimentation velocity profiles of the N-βGRP−laminarin complex with increasing amounts of laminarin. This material is available free of charge via the Internet at http://pubs.acs.org.

Accession Codes

Atomic coordinates have been deposited into the Protein Data Bank as entry 2KHA.

■ AUTHOR INFORMATION

Corresponding Author

*Department of Biochemistry, Kansas State University, Manhattan, KS 66506. Telephone: (785) 532-6262. Fax: (785) 532-7278. E-mail: krish@ksu.edu.

Present Addresses

§Division of Chemistry and Chemical Engineering, California Institute of Technology, Pasadena, CA 91125.

‖USDA-ARS, U.S. Arid Land Agricultural Research Center, Maricopa, AZ 85238.

Author Contributions

H.D. and Y.H. contributed equally to this work.

Notes

The authors declare no competing financial interest.

■ ABBREVIATIONS

βGRP, β-1,3-glucan recognition protein; GNBP, Gram-negative bacteria binding protein; NMR, nuclear magnetic resonance; ITC, isothermal titration calorimetry; AUC, analytical ultracentrifugation; SDS–PAGE, sodium dodecyl sulfate–polyacrylamide gel electrophoresis; proPO, prophenoloxidase; PDB, Protein Data Bank.

■ REFERENCES

(1) Ochiai, M., and Ashida, M. (2000) A pattern-recognition protein for β-1,3-glucan. The binding domain and the cDNA cloning of β-1,3-glucan recognition protein from the silkworm, *Bombyx mori. J. Biol. Chem. 275,* 4995−5002.

(2) Ma, C., and Kanost, M. R. (2000) A β-1,3-glucan recognition protein from an insect, *Manduca sexta,* agglutinates microorganisms and activates the phenoloxidase cascade. *J. Biol. Chem. 275,* 7505−7514.

(3) Kim, Y. S., Ryu, J. H., Han, S. J., Choi, K. H., Nam, K. B., Jang, I. H., Lemaitre, B., Brey, P. T., and Lee, W. J. (2000) Gram-negative bacteria-binding protein, a pattern recognition receptor for lipopolysaccharide and β-1,3-glucan that mediates the signaling for the induction of innate immune genes in *Drosophila melanogaster* cells. *J. Biol. Chem. 275,* 32721−32727.

(4) Fabrick, J. A., Baker, J. E., and Kanost, M. R. (2003) cDNA cloning, purification, properties, and function of a β-1,3-glucan recognition protein from a pyralid moth, *Plodia interpunctella. Insect Biochem. Mol. Biol. 33,* 579−594.

(5) Jiang, H., Ma, C., Lu, Z. Q., and Kanost, M. R. (2004) β-1,3-glucan recognition protein-2 (βGRP-2)from *Manduca sexta*; an acute-phase protein that binds β-1,3-glucan and lipoteichoic acid to aggregate fungi and bacteria and stimulate prophenoloxidase activation. *Insect Biochem. Mol. Biol. 34,* 89−100.

(6) Gottar, M., Gobert, V., Matskevich, A. A., Reichhart, J. M., Wang, C., Butt, T. M., Belvin, M., Hoffmann, J. A., and Ferrandon, D. (2006) Dual detection of fungal infections in *Drosophila* via recognition of glucans and sensing of virulence factors. *Cell 127,* 1425−1437.

(7) An, C., Ishibashi, J., Ragan, E. J., Jiang, H., and Kanost, M. R. (2009) Functions of *Manduca sexta* hemolymph proteinases HP6 and HP8 in two innate immune pathways. *J. Biol. Chem. 284,* 19716−19726.

(8) Roh, K. B., Kim, C. H., Lee, H., Kwon, H. M., Park, J. W., Ryu, J. H., Kurokawa, K., Ha, N. C., Lee, W. J., Lemaitre, B., Söderhäll, K., and Lee, B. L. (2009) Proteolytic cascade for the activation of the insect toll pathway induced by the fungal cell wall component. *J. Biol. Chem. 284,* 19474−19481.

(9) Fabrick, J. A., Baker, J. E., and Kanost, M. R. (2004) Innate immunity in a pyralid moth: Functional evaluation of domains from a β-1,3-glucan recognition protein. *J. Biol. Chem. 279,* 26605−26611.

(10) Matskevich, A. A., Quintin, J., and Ferrandon, D. (2010) The *Drosophila* PRR GNBP3 assembles effector complexes involved in antifungal defenses independently of its Toll-pathway activation function. *Eur. J. Immunol. 40,* 1244−1254.

(11) Takahasi, K., Ochiai, M., Horiuchi, M., Kumeta, H., Ogura, K., Ashida, M., and Inagaki, F. (2009) Solution structure of the silkworm βGRP/GNBP3 N-terminal domain reveals the mechanism for β-1,3-glucan-specific recognition. *Proc. Natl. Acad. Sci. U.S.A. 106,* 11679−11684.

(12) Kanagawa, M., Satoh, T., Ikeda, A., Adachi, Y., Ohno, N., and Yamaguchi, Y. (2011) Structural insights into recognition of triple-helical β-glucans by an insect fungal receptor. *J. Biol. Chem. 286,* 29158−29165.

(13) Mishima, Y., Quintin, J., Aimanianda, V., Kellenberger, C., Coste, F., Clavaud, C., Hetru, C., Hoffmann, J. A., Latge, J. P., Ferrandon, D., and Roussel, A. (2009) The N-terminal domain of *Drosophila* Gram-negative binding protein 3 (GNBP3) defines a novel family of fungal pattern recognition receptors. *J. Biol. Chem. 284,* 28687−28697.

(14) Hrmova, M., and Fincher, G. B. (1993) Purification and properties of three (1−3)-β-D-glucanase isoenzymes from young leaves of barley (*Hordeum vulgare*). *Biochem. J. 289,* 453−461.

(15) Handa, N., and Nisizawa, K. (1961) Structural investigation of a laminaran isolated from *Eisenia bicyclis. Nature 192,* 1078−1080.

(16) Delaglio, F., Grzesiek, S., Vuister, G. W., Zhu, G., Pfeifer, J., and Bax, A. (1995) NMRPipe: A multidimensional spectral processing system based on UNIX pipes. *J. Biomol. NMR 6,* 277−293.

(17) Goddard, T. D., and Kneller, D. G. (2001) *SPARKY 3,* University of California, San Francisco.

(18) Cavanagh, C., Palmer, A. G., III, and Skelton, N. J. (1996) *Protein NMR Spectroscopy: Principles and Practice,* Academic Press, San Diego.

(19) Cornilescu, G., Delaglio, F., and Bax, A. (1999) Protein backbone angle restraints from searching a database for chemical shift and sequence homology. *J. Biomol. NMR 13,* 289−302.

(20) Wishart, D. S., Sykes, B. D., and Richards, F. M. (1992) The chemical shift index: A fast and simple method for the assignment of protein secondary structure through NMR spectroscopy. *Biochemistry 31,* 1647−1651.

(21) Brünger, A. T., Adams, P. D., Clore, G. M., DeLano, W. L., Gros, P., Grosse-Kunstleve, R. W., Jiang, J. S., Kuszewski, J., Nilges, M., Pannu, N. S., Read, R. J., Rice, L. M., Simonson, T., and Warren, G. L. (1998) Crystallography & NMR system: A new software suite for macromolecular structure determination. *Acta Crystallogr. D54,* 905−921.

(22) Hiromasa, Y., Fujisawa, F., Aso, Y., and Roche, T. E. (2004) Organization of the cores of the mammalian pyruvate dehydrogenase complex formed by E2 and E2 plus the E3-binding protein and their capacities to bind the E1 and E3 components. *J. Biol. Chem. 279,* 6921−6933.

(23) Perkins, S. J., Miller, A., Hardingham, T. E., and Muir, H. (1981) Physical properties of the hyaluronate binding region of proteoglycan from pig laryngeal cartilage: Densitometric and small-angle neutron scattering studies of carbohydrates and carbohydrate-protein macromolecules. *J. Mol. Biol. 150,* 69−95.

(24) Wiseman, T., Williston, S., Brandts, J. F., and Lin, L. N. (1989) Rapid measurement of binding constants and heats of binding using a new titration calorimeter. *Anal. Biochem. 179,* 131−137.

(25) Laughton, A. M., and Siva-Jothy, M. T. (2011) A standardised protocol for measuring phenoloxidase and prophenoloxidase in the honey bee, *Apis mellifera. Apidologie 42,* 140−149.

(26) Clore, G. M., and Gronenborn, A. M. (1994) Multidimensional heteronuclear nuclear magnetic resonance of proteins. *Methods Enzymol. 239*, 349−363.

(27) Peng, J. W., and Wagner, G. (1994) Investigation of protein motions via relaxation measurements. *Methods Enzymol. 239*, 563−596.

(28) Amzel, L. M., and Poljak, R. J. (1979) Three-dimensional structure of immunoglobulins. *Annu. Rev. Biochem. 48*, 961−997.

(29) Okuyama, K., Otsubo, A., Fukuzawa, Y., Ozawa, M., Harada, T., and Kasai, N. (1991) Single helical structure of native Curdlan and its aggregation state. *Carbohydr. Chem. 10*, 645−656.

(30) Deslandes, Y., Marchessault, R. H., and Sarko, A. (1980) Triple-helical structure of (1−3)-β-D-glucan. *Macromolecules 13*, 1466−1471.

(31) Barral, P., Suarez, C., Batanero, E., Alfonso, C., Alche Jde, D., Rodriguez-Garcia, M. I., Villalba, M., Rivas, G., and Rodriguez, R. (2005) An olive pollen protein with allergenic activity, Ole e 10, defines a novel family of carbohydrate-binding modules and is potentially implicated in pollen germination. *Biochem. J. 390*, 77−84.

(32) Young, S. H., Dong, W. J., and Jacobs, R. R. (2000) Observation of a partially opened triple-helix conformation in 1→3-β-glucan by fluorescence resonance energy transfer spectroscopy. *J. Biol. Chem. 275*, 11874−11879.

(33) Schachman, H. K. (1959) *Ultracentrifugation in Biochemistry*, Academic Press, New York.

(34) Boraston, A. B., Bolam, D. N., Gilbert, H. J., and Davies, G. J. (2004) Carbohydrate-binding modules: Fine-tuning polysaccharide recognition. *Biochem. J. 382*, 769−781.

(35) Hiromasa, Y., and Roche, T. E. (2003) Facilitated interaction between the pyruvate dehydrogenase kinase isoform 2 and the dihydrolipoyl acetyltransferase. *J. Biol. Chem. 278*, 33681−33693.

(36) Wang, Y., and Jiang, H. (2006) Interaction of β-1,3-glucan with its recognition protein activates hemolymph proteinase 14, an initiation enzyme of the prophenoloxidase activation system in *Manduca sexta. J. Biol. Chem. 281*, 9271−9278.

(37) Buchon, N., Poidevin, M., Kwon, H. M., Guillou, A., Sottas, V., Lee, B. L., and Lemaitre, B. (2009) A single modular serine protease integrates signals from pattern-recognition receptors upstream of the *Drosophila* Toll pathway. *Proc. Natl. Acad. Sci. U.S.A. 106*, 12442−12447.

(38) Lim, J. H., Kim, M. S., Kim, H. E., Yano, T., Oshima, Y., Aggarwal, K., Goldman, W. E., Silverman, N., Kurata, S., and Oh, B. H. (2006) Structural basis for preferential recognition of diaminopimelic acid-type peptidoglycan by a subset of peptidoglycan recognition proteins. *J. Biol. Chem. 281*, 8286−8295.

(39) Weis, W. I., and Drickamer, K. (1996) Structural basis of lectin-carbohydrate recognition. *Annu. Rev. Biochem. 65*, 441−473.